Artigo

SYNTHESIS AND THEORETICAL STUDY OF HPW CATALYSTS SUPPORTED ON NIOBIA CALCINATED AT 500 AND 600 °C

Claudia V. Lacerda[a,#], Livia C. T. Lacerda[b], Alexandre A. de Castro[b], Tanos C. C. França[a,c,*], Teodorico C. Ramalho[b,c], Nadine Essayem[d] and Wilma de A. Gonzalez[a,]**

[a]Seção de Engenharia Química, Instituto Militar de Engenharia, 22290-270 Rio de Janeiro – RJ, Brasil

[b]Departamento de Química, Universidade Federal de Lavras, 3720-000 Lavras – MG, Brasil

[c]Department of Chemistry, Faculty of Science, University of Hradec Kralove, 500 03 Hradec Králové – Czech Republic

[d]Institut des Recherches sur la Catalyse et l'Environnement de Lyon, 69626 Villeurbanne – France

Recebido em 08/04/2019; aceito em 11/06/2019; publicado na web em 11/07/2019

Keggin heteropolyacids (HPW) supported on niobia have been considered for both homogeneous and heterogeneous catalysis due to its special features, like the strong Brönsted acidity, low volatility, high activity and high selectivity for various reactions in comparison with mineral acids. Literature reports many different preparation methods for these catalysts through the addition of HPW solutions, in either water or acid, over niobia under stirring. However not much is known about the way how HPW interacts with the support, neither how the temperature influences this interaction. In order to contribute to expand the knowledge on this field we report here a new way of preparing HPW supported catalysts over niobia calcined at 500 and 600 °C, followed by a theoretical study meant to check the influence of the temperature increase on the adsorption behavior of the catalysts over the support. Our proposed method showed to be an efficient alternative for impregnation of HPW over niobia, while the theoretical results suggest that pseudo-hexagonal and orthorhombic are the most likely crystalline forms for these catalysts.

Keywords: HPW; niobia; theoretical study.

INTRODUCTION

Keggin's type heteropolyacids consist of 12 tungsten or molybdenum ions (called polyatoms) and oxygen atoms arranged symmetrically around a central P atom (called heteroatom), which chemical formula is $[X^{n+}M_{12}O_{40}]^{(8-n)}$.[1-9] Literature reports the solid heteropolyacids in several hydrated forms, dependent on the level of hydration, which is defined by temperature and humidity. The most hydrated one presents around 30 water molecules in a quite cubic open structure, containing protons and zeolitic water. Lattice changes happen when dehydration occurs.[10-15]

The polyacid have an important characteristic related to their low charge density at the spherical surface of the molecule, avoiding localized charges. The protons are mobile, resulting in a strong Brönsted acidity. They also exhibit low volatility, high activity and high selectivity for various reactions when compared to mineral acid.[2,5] Due to these features such compounds are used for both homogeneous as well as heterogeneous catalysis,[10-16] providing greater efficiency and a cleaner process.[17] However, Keggin's type (HPWs) have the disadvantage of presenting low thermal stability and specific surface area (1-10 $m^2\ g^{-1}$), and solubility in polar medium.[18-20] These inconveniences could be mitigated by impregnating the HPW on supports in order to prevent leaching of the catalyst in the presence of polar solvents, and enhance the catalytic performance. According to the literature, the increase in catalytic activity is due to the strong adsorption of protons from HPW on supports like alumina,[21-23] titania,[21,24-26] activated carbon,[27,28] MCM-41,[29,30] acidic ion exchange resins,[31] clays,[21,32,33] silica,[27,34,35] and zirconia.[24,36,37]

It has been found that the use of $Nb_2O_5.xH_2O$ (hydrated niobium oxide), also known as niobia, as support for the Keggin ion, showed interesting results.[38-40] Due to these results and the fact that Nb is an abundant mineral in Brazilian territory, niobia has been seen as an interesting low cost and, eventually more efficient, option as support to HPW by the Brazilian scientific community. Having this in mind and willing to contribute to deepen the understanding on the interactions between HPW and the support, we prepared, using a new method of preparation, niobia supported HPW catalysts using 30%, 50% and 100%, respectively, of HPW supported over calcined niobia at 500 and 600 °C, temperatures not tried before in literature. The reasoning behind this choice was to investigate the possibility of synthesizing these catalysts at these conditions, once it's known that, at such temperatures, Lewis sites could be formed over the surface, fact that would broaden the possibilities of application of these catalysts. Also, considering that few theoretical studies are available in literature,[41-44] we further performed an unprecedented theoretical study in order to check the influence of the temperature increase on the adsorption behavior of the catalysts over the niobia surface.

EXPERIMENTAL

Impregnation and heat treatment

Niobium oxide hydrated, $Nb_2O_5.xH_2O$, code HY340, provided by CBMM (Brazilian Society of Mining and Metallurgy), was used as support for the impregnation of the catalysts.

The impregnation was made on the support with previous calcination at 500 °C and 600 °C for 2 h at 2 °C min^{-1} under N_2 flow. Before impregnation, the catalyst was maintained at 80 °C for 1 h in a rotary evaporator. Then, the systems were cooled to room temperature and the required amount of aqueous solution containing 30%, 50% and 100% of $H_3PW_{12}O_{40}.nH_2O$ (Sigma-Aldrich) was added dropwise, under constant stirring. After impregnation, the catalysts were maintained under agitation for 1 h and, then, frozen during 24 h and freeze-dried following the same procedure adopted before in a former work.[45]

*e-mail: tanos@ime.eb.br; **e-mail: d5wilma@gmail.com

#alternative e-mail: cvlacerda.cl@gmail.com

The catalysts were named 30HPW/Nb500 and 30HPW/Nb600 for the catalysts with 30% HPW supported on niobia calcined at 500 and 600 °C, respectively; 50HPW/Nb500 and 50HPW/Nb600 for the catalysts with 50% HPW supported on niobia calcined at 500 and 600 °C, respectively; and 100HPW/Nb500 and 100HPW/Nb600 for the catalysts with 100% HPW supported on niobia calcined at 500 and 600 °C, respectively.

Characterization

The surface areas were determined through N_2 adsorption. Samples were desorbed in cell BET under vacuum at 150 °C for 5h with a ramp of 5 °C/min and analyzed in ASAP 2020 from Micromeritics, V1.05 G unit 1. The X-ray diffraction (XRD) patterns in θ-2θ of the samples, without previous treatment, were performed on a Siemens diffractometer using radiation Cu Kα at room temperature.

Infrared (FTIR) were recorded with a Bruker Vector 22 spectrophotometer. The samples were mixed with dried KBr, forming pellets containing 1 wt% and the spectra were taken with 32 scans at 4 cm^{-1} of resolution.

For FT-Raman we used a Linkam TS1500 cell spectrophotometer. The spectra were recorded under ambient conditions, with 128 scans, wavelength of 514nm and a 50x objective.

The ^{31}P MAS-NMR spectra were acquired using a spectrometer Bruker DSX400 equipped with a standard 4 mm triple resonance probe H-X-Y. The spinning rate was typically 10 KHz and the repetition time was 60s. The samples were analyzed without pretreatment.

Theoretical studies

This theoretical investigation aimed to analyze the influence of the increased calcination temperature on HPW adsorption, and examine which factors are involved. Above the calcination temperatures, in which crystal structures of Nb_2O_5 are found, three phases were selected to perform the theoretical calculations: phase TT and T (from 450 °C to 600 °C), and phase B (800 °C). These Nb_2O_5 phases were chosen to perform the calculation procedures due to the availability of crystallographic parameters which allowed for the construction of the model. The goal of this investigation was to evaluate the change in the adsorption behavior with increasing the temperature of calcination of the material on the catalysts modeling, considering the influences of hydrogen atoms on the surface of the support in the HPW adsorption. For the construction of the calcined niobia the crystallographic parameters shown in Table 1 were employed.

The crystal structures of the calcined niobia were constructed (phases TT, T and B) by using the ADF software, (Amsterdam Density Functional) – BAND 2009, where the faces of each structure (phase) were analyzed, through the Density Functional Theory (DFT) method, at the GGA – PBE level. For the correction of density gradient for the exchange and correlation function, it was used a set of TZP basis. HPW was introduced on each face with a subsequent optimization and identification of the minimum energy, checking the symmetry of the calcined niobia. This procedure allowed us to figure out the favorable regions of interaction between niobia and HPW. The structures were optimized by using the ADF program with the Vosko-Wilk-Nusair generalized approximation gradient (GGA/PW91) for density gradient correction to the exchange and correlation function.[46] It was used the TZP basis set for this procedure, since the relativistic effects are considered important for certain atoms, such as tungsten. Thus, the calculations were performed within the relativistic scheme with the zero-order regular approach (ZORA) in order to include scalar effects.[46] The HPW adsorption was evaluated by introducing it into two different positions in the planes (001) of each phase, TT, T and B-Nb_2O_5, in order to check out the most favorable regions of interaction. The adsorption energy of the HPW on the niobia surface was calculated according to equation 1.

$$\Delta E_{ads} = E_{sys} - [E_{Nb_2O_5} + E_{HPW}] \quad (1)$$

where ΔE_{ads} is the adsorption energy; E_{sys} is the energy of the system after adsorption and E_{Nb2O5} and E_{HPW} are the energies of the isolated structures. After optimizing the structures, an analysis of how the hydroxyl groups on the hydrogenated surface influence the HPW adsorption on the calcined niobia was performed.[46] In order to carry out this analysis, the hydrogenated surface of niobia was simulated by adding hydroxyl groups over the plane (001) of phase TT, followed by an optimization process. This analysis was important to provide us a better comprehension of the good HPW adsorption in amorphous phases, in comparison to crystalline phases. The ΔE_{ads} was computed according to equation 1.

With regards to electronic-structure investigations, it is observed an increased number of works that involve the Hubbard term to the local density approximation band-structure Hamiltonian.[47] For instance, this theory is commonly employed in order to minimize the total ground-state energy of the electrons in a material, being important for transition metals. The Hubbard model term is a static Coulomb interaction for frozen orbitals, preventing the average energy of the correlated orbitals from being pushed too high by fitting the correct average occupation of the correlated orbitals.[48] This is a quite useful approach, but for these HPW adsorption studies on niobia, its effect is not so relevant for the systems in study.

A further analysis was performed in order to evaluate better the hydrogen's situation and strength after the structures minimization. One of the most useful tools to characterize atomic and molecular interactions, for example hydrogen bonds, is the topological analysis using the "atoms in molecules" (AIM) theory,[49] a technique used to analyze the electron density and nature of the bonds in molecular structures. According to the AIM theory, any chemical bonding is characterized by the existence of a bond critical point (BCP). After the optimization calculations it was performed an analysis of the H-bonds between HPW and niobia through the quantum theory of atoms and molecules (QTAIM) method.[50]

RESULTS AND DISCUSSION

Powder X-ray diffraction (XRD)

The diffractograms in Figure 1 show that catalysts 30HPW/Nb500 and 50HPW/Nb500 presented amorphous structures, suggesting a

Table 1. Experimental crystallographic parameters (phases B and T) and calculated crystallographic parameters (phase TT) for niobia

Phase	Space group	a (Å)	b (Å)	c (Å)	b (°)	Ω (Å^3)	References
B	*C2/c*	12.740(2)	4.8830(6)	5.5609(6)	105.02(1)	334.11	[38]
T	*Pbam*	6.175(1)	29.175(4)	3.930(1)	--	708.01	[39]
TT	*P6/mmm*	7.191	7.191	3.831	--	171.56	[40]

good dispersion of HPW over the support, while catalyst 100HPW/Nb500 presented low intensity rays, pointing to the presence of crystalline HPW at 10, 26 and 35° over the support's surface. Catalysts 30HPW/Nb600, 50HPW/Nb600 and 100HPW/Nb600, on the other hand, presented diffractograms characteristics of niobia with hexagonal structure, due to the change from the amorphous phase to TT-Nb_2O_5 and/or T-Nb_2O_5, corresponding to the pseudo-hexagonal and/or orthorhombic structures.[47] These results are in accordance with the observations by Jehng and Wachs[51] regarding the increase in the degree of crystallinity of the amorphous niobia during the thermal treatment at temperatures in the range of 300 to 1000 °C, transforming them in more stable phases.[51]

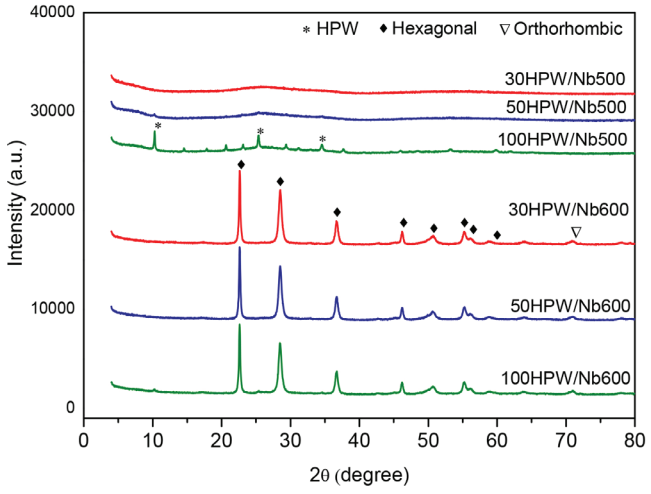

Figure 1. *XRD patterns of the catalysts*

Surface area (BET) determination

As can be seen in Table 2, the increase in the calcination temperature lead to a gradual reduction of the specific areas for both support and catalyst. For niobia this reduction was probably caused by the increase in crystallinity due to the phase change from the amorphous oxide to its crystalline phases with hexagonal or orthorhombic structures, as discussed before. For the catalysts, we believe that this reduction in specific area was provoked by the presence of HPW, as well as the variation on its content in the catalysts, besides the increase in the calcination temperature.

Table 2. BET specific areas for support and catalysts

T (°C)	Surface area ($m^2\ g^{-1}$)			
	Support	30HPW/Nb	50HPW/Nb	100HPW/Nb
25	144	-	-	-
500	99	90.7	86.1	68.2
600	23	25.4	24.1	23.1

FT-IR spectroscopy

In the FT-IR studies we performed comparisons in order to verify the influence of content and temperature on the superficial properties of the catalysts. For all analysis pure $H_3PW_{12}O_{40}.6H_2O$, treated at 100 °C, and niobia at 25 °C (Nb25), were used as references. As shown in Table 3, the HPW presented vibrations in accordance with the results reported by Kozhevnikov *et al.*[52]

In both spectra, for catalysts and the reference samples (HPW and niobia), signals at ~1630 cm^{-1} were observed. This band can indicate the presence of the $H_5O_2^+$ (hydroxonions), which binds 4 Keggin units, forming the secondary structure, or can be a characteristic peak of the niobia at ~1623 cm^{-1}, resulting from the angular deformation of the water molecules adsorbed, thus confirming the presence of water molecules physiosorbed in the samples (see Table 3 and Figure 2).

The FT-IR spectra in Figure 2 show that the catalysts calcined at 500°C were more resistant to the temperature variation, once the shape of the spectra resembles the HPW's, with a more accentuated interference of the Nb bands between 400-800 cm^{-1}. The peaks corresponding to HPW were more intense for the catalyst 100HPW/Nb500, due to the higher content of HPW.

For catalysts 30HPW/Nb600, 50HPW/Nb600 and 100HPW/Nb600, prevailed the bands corresponding to niobia, probably due to the structural change reported before in the DRX analysis (Figure 1). The catalyst 100HPW/Nb600 presented a discrete signal around ~ 1081 cm^{-1}, attributed to the vibration ϑ_{as}(P-O_a), analogue to HPW.

For both calcination temperatures it was not possible to identify the peak corresponding to the deformation (O-P-O) in the region around 595 cm^{-1}. We believe that this was due to an overlapping of the niobia bands present in the region around 400-600 cm^{-1} from the vibrations of the type Nb-O_p-Nb, in bridge shape.[53] Considering that the DRX analysis (Figure 1) has shown the presence of HPW, we believe that there was an overlapping of the FT-IR signals from HPW and niobia.

Table 3. FT-IR vibrational modes for support and catalysts

	ϑ_s(W-O-W)	δ(O-P-O)	ϑ_{as}(W-O_e-W)	ϑ_{as}(W-O_c-W)	ϑ_{as}(W=O_t)	ϑ_{as}(P-O_a)	$\delta(H_5O_2^+)$ for HPW and ϑ_{bend}(HOH) water for Nb25	Nb-Op-Nb	ϑNb-O	ϑNb=O
	Frequency (cm^{-1})									
$H_3PW_{12}O_{40}.6H_2O$	525	596	800	887	986	1080	1628	-	-	-
Nb25	-	-	-	-	-	-	1623	498	633	912
30HPW/Nb500	-	-	808	890	-	1077	1627	-	-	-
50HPW/Nb500	-	-	803	885	978	1077	1615	-	-	-
100HPW/Nb500	522	-	-	889	983	1081	1625	-	-	-
30HPW/Nb600	-	618	-	882	-	1174	-	459	-	-
50HPW/Nb600	-	604	820	882	-	1074	1616	-	-	-
100HPW/Nb600	-	607	814	881	-	1081	1623	-	-	-

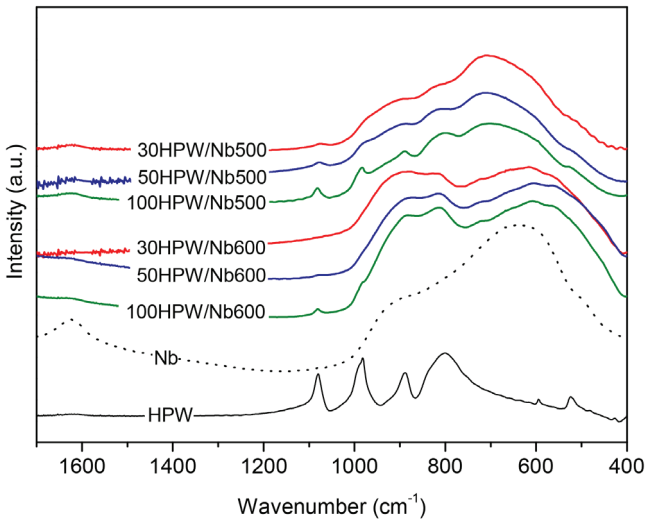

Figure 2. *FT-IR spectra of the catalysts calcined at 500 and 600 °C*

FT-Raman spectroscopy

The results obtained through FT-Raman spectroscopy were evaluated by comparing the contents of HPW added to the support and the variation in the temperatures of calcination. The respective spectra and frequencies are presented in Figure 3 and Table 4.

According to the literature[43] the FT-Raman spectra of HPW present vibrations related to the respective structural bonds at 1100, 990, 900 and 550 cm^{-1}, corresponding to: P-O stretch, symmetric vibration $_{\vartheta s}(W{=}O_t)$, and deformations W-O_c-W and O-P-O, respectively. Figure 3 shows the symmetric vibration $_{\vartheta s}(W{=}O_t)$ at ~1006 cm^{-1}, for concentrations 30 and 50% and at ~1010 cm^{-1} for 100% of HPW content for the samples calcined at 500 °C. The catalyst 100HPW/Nb500, presented a small shoulder at ~906 cm^{-1} originated from vibration (W-O_c-W) as also observed by Khder *et al.*[54] The bands between 700-800 cm^{-1} were not detected, probably because they are overlapped by the support bands in this region. The bands at 220 and 665 cm^{-1}, referring to intact HPW over the support surface, are present in these catalysts.

The catalyst 100HPW/Nb600 presented the vibration $_{\vartheta s}(W{=}O_t)$ at ~1029 cm^{-1}. This shift related to the former catalysts is probably due to the temperature of calcination. For catalysts 30HPW/Nb600 and 50HPW/Nb600, it was not possible to detect, through the Raman spectra (Figure 3), the signals related to the presence of HPW.

The FT-Raman spectra presented also the characteristic bands of niobia with absorption between 850-1000 cm^{-1}, corresponding to the octahedral structure of NbO_6 highly distorted with bonds Nb=O terminals.[55,56] The bond Nb-O present in the region around 500-700 cm^{-1}, belongs to the octahedral structure slightly distorted of NbO_6. This bond is also present in species NbO_7 and NbO_8.[56] According to Jehng and Wachs[51] the bands between 400-800 cm^{-1} are attributed to the symmetric and asymmetric stretching modes of the bonds Nb-O-Nb, and its associated deforming modes show up in the region of low wave length, between 200-300 cm^{-1}. We believe that the signal around ~180 cm^{-1} has been shifted due to the presence of HPW.

According to Janik *et al.*,[57] HPW loses crystallization water at low temperatures (<200°C). From this temperature over, the water lost is due to the deprotonation of the acid. So, at 600°C, probably the species present in the solid are Nb_2O_5, WO_3 and P_2O_5.

As in the FT-IR study (Figure 2), it was not possible to detect the signal $_{\vartheta s}(W{=}O_t)$, which confirms the presence of HPW, for the catalysts 30HPW/Nb600 and 50HPW/Nb600 in the FT-Raman spectra (Figure 3).

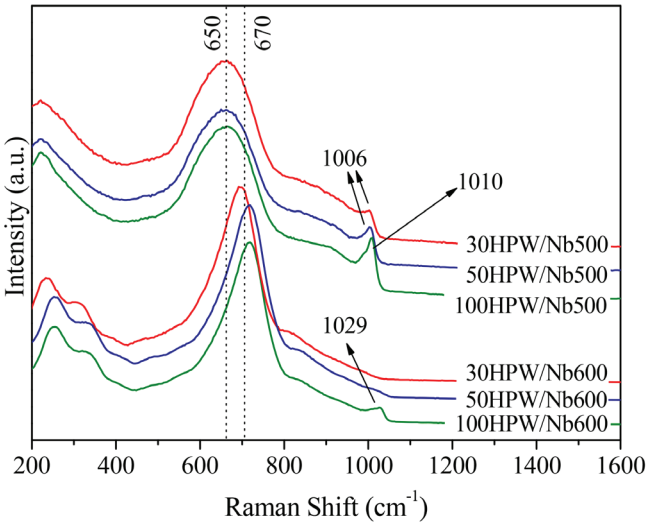

Figure 3. *FT-Raman spectra of the catalysts*

^{31}P MAS NMR

According to Kumar *et al.*,[40] an appropriate and very efficient method to elucidate the structure and check the stability of HPW is the solid state ^{31}P NMR spectroscopy, once features like purity and degree of hydration change in the environment around the transition metal central atom and formation of $[\equiv M{-}OH_2]n + [H_{3-n}]^{n-3}$ species are due to interactions between the support and the HPW.

Our ^{31}P MAS RMN results confirmed the presence of HPW over the support, suggesting that our impregnation method was efficient. In the ^{31}P NMR spectra, presented in Figure 4, it's possible to see that, except for catalysts 30HPW/Nb600 and 100HPW/Nb600, there are 2 different chemical environments for ^{31}P. In the spectra for catalysts calcined at 500 °C and for catalyst 50HPW/Nb600, there is the signal around –14.3 ppm, suggesting that the HPW is strongly adsorbed to

Table 4. Frequency (cm^{-1}) of FT-Raman spectra of the catalysts

HPW	-	-	-	-	-	-	550	-	-	-	900	990	-	1100
Nb25	205	-	-	-	-	-	-	657	-	-	884	-	-	-
30HPW/Nb500	-	221	-	-	-	-	-	665	-	-	-	-	1006	-
50HPW/Nb500	-	221	-	-	-	-	-	650	-	-	-	-	1006	-
100HPW/Nb500	-	221	-	-	-	-	-	665	-	-	906	-	1010	-
30HPW/Nb600	-	-	233	-	312	-	-	-	692	822	-	-	-	-
50HPW/Nb600	-	-	-	253	-	335	-	-	719	838	-	-	-	-
100HPW/Nb600	-	-	-	257	-	335	-	-	719	831	-	-	1029	-

the support, due to the enlargement of the peak between the HPW species, finely dispersed over the support.[58]

The signal around –13.0 ppm (for 30HPW/Nb500 and 50HPW/Nb500) is characteristic of HPW weakly adsorbed, without decomposition of the Keggin anion through thermic treatment[34] or due to distorted species of HPW interacting with the support. As observed by Kozhevnikov *et al.*,[58] these species could be poly condensate materials of PW_9.

All catalysts calcined at 500 °C and the catalyst 50HPW/Nb600, presented the peaks at –14.3, –14.4 e –14.6 ppm characteristics of $[PW_{12}O_{40}]^{3-}$, suggesting a strong adsorption due to the enlargement of the peak between the HPW species.[58] One signal of low intensity at -15 ppm, was observed for the catalyst 30HPW/Nb600, and former attributed by Essayem *et al.*[59] and Uchida *et al.*[60] to the crystalline HPW where all poly-anions are equally H-bonded through the $H_5O_2^+$, former visualized in the FT-IR spectra at ~1630 cm^{-1} (Figure 2).

In the spectrum of catalyst 50HPW/Nb600 we can also see the signal at 1.0 ppm corresponding to the presence of the orthophosphate diester, which is apparently a flaw in the HPW structure provoked by the rising of the temperature. The signals at –14.4 and –16 ppm observed for catalyst 100HPW/Nb500 can be attributed, respectively to the species $[PW_{12}O_{40}]^{-3}$ and to the presence of the Keggin unit.[37]

Catalyst 100HPW/Nb600 presented one single peak centered at –15.5 ppm, typical of intact HPW, that would be strongly adsorbed over the niobia surface. Mastikhin *et al.*[61] propose that the presence of this signal suggests distortion in the crystalline structure, probably due to the presence of flaws in the HPW crystals deposited in pores of the support.

Theoretical studies

For the HPW adsorption on different phases, the acid was introduced into two different positions in the faces (001) of each phase (Figure 5). In position 1, HPW was placed so that all hydrogen atoms stay as far as possible from the surface. On the other hand, in position 2, one of the hydrogen atoms in HPW directly interacts with the surface.

The HPW geometries in contact with the crystalline phases of the niobia were optimized and the final electronic energy of the system was obtained. Table 5 shows the relative energies of the adsorbed systems.

The increase of the calcination temperature of polymorphic materials yields increasingly crystalline phases. For the niobia, by increasing the calcination temperature, the first crystalline phase to appear is TT (pseudohexagonal), which generally takes place from 450 °C, followed by phase T (orthorhombic), around 600 °C and phase B (Monoclinic), around 800 °C.[37] The theoretical results have shown that the system with the adsorbed acid on the TT-Nb_2O_5 phase surface is more stable, followed by T-Nb_2O_5 and B-Nb_2O_5, respectively. An increased energy is then related, with the increasing of the material crystallinity and, according to these data, the adsorption process is favored in milder conditions of temperature, with HPW being better adsorbed in phase TT.

The direct interaction of the hydrogen with oxygen atoms on the surface, held in position 2, could lead to stronger and more stable interactions. Surprisingly, the adsorption when HPW is in position 1 is more favorable compared to position 2 for all phases. In view of this scenario, the higher instability of the Nb_2O_5/HPW(pos2) system, in relation to Nb_2O_5/HPW(pos1), may be due to steric effects present between the surface and HPW(pos2), overcoming the influence of the hydrogen interaction performed. This can be inferred due to the fact that the minimum energy of HPW adsorption on this disposal takes place at upper distances in relation to position 1 (Table 6).

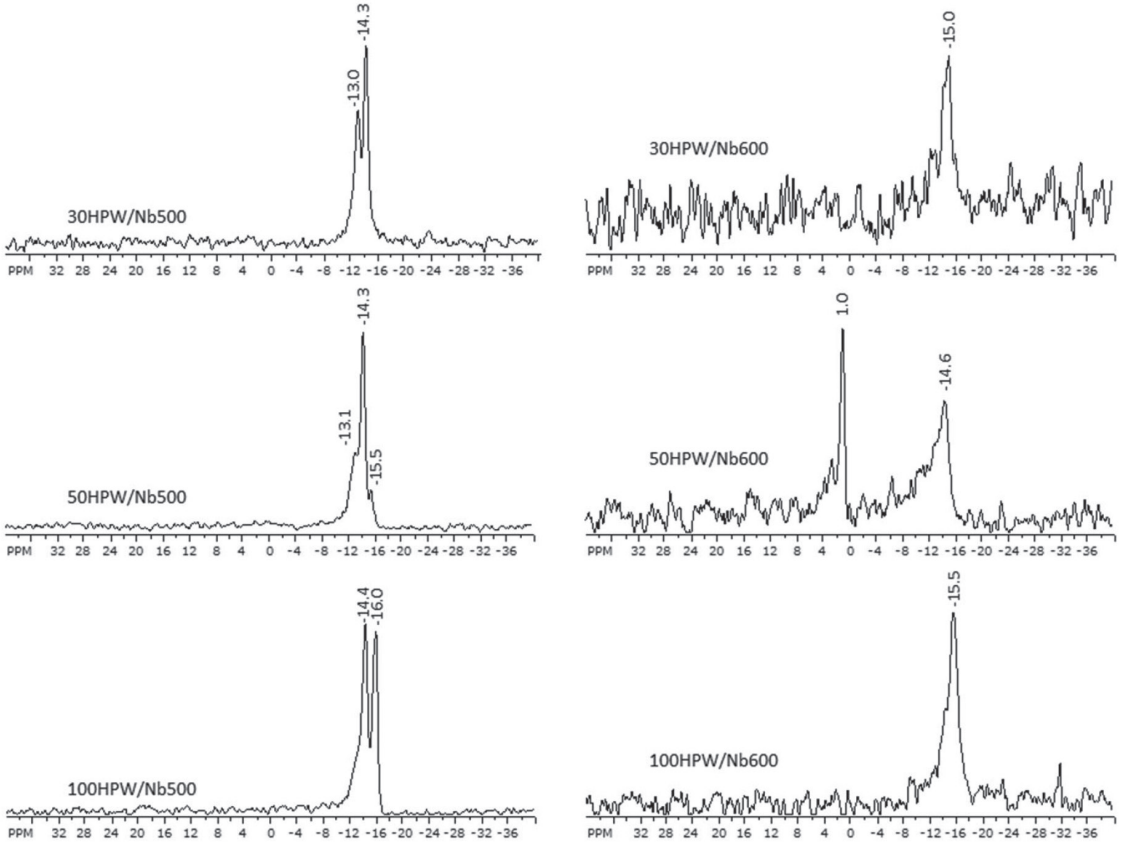

Figure 4. *[31]P MAS NMR spectra of the catalysts*

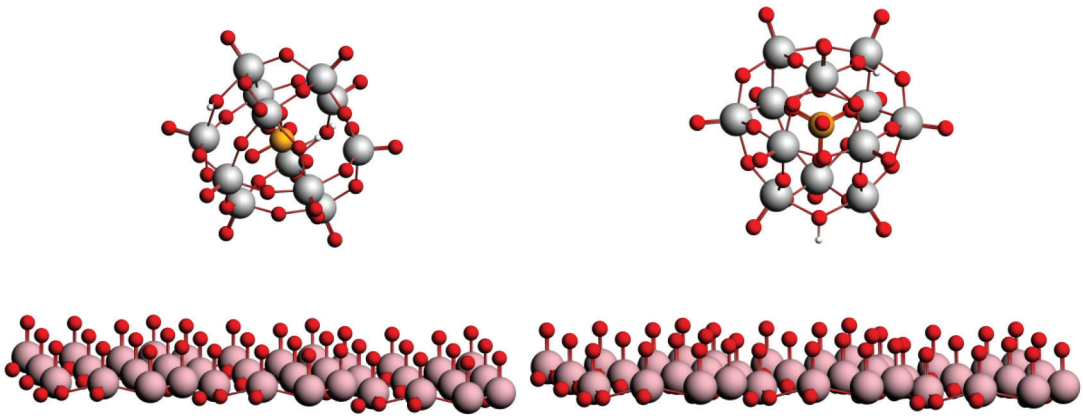

Figure 5. *Illustration of the HPW adsorption on the TT-Nb_2O_5 phase in position 1 (left): Nb_2O_5/HPW (pos1), and position 2 (right): Nb_2O_5/HPW (pos2). Red: oxygen, pink: niobium, gray: tungsten, orange: phosphorus, white: hydrogen*

Table 5. Relative adsorption energies (Er_{ads}), in kcal mol^{-1}, for the adsorbed HPW on dehydrogenated phases

Phase	$Er_{ads}(pos1)$	$Er_{ads}(pos2)$
TT	0	15.90
T	30.19	40.11
B	42.42	49.18

Table 6. Distances (in Å) between the surfaces and HPW relating to the geometry of the minimum energy of adsorption

Phase	$d_{S\text{-}HPW}(A)$ $(pos1)$	$d_{S\text{-}HPW}(A)$ $(pos2)$
TT	3.29	4.08
T	3.20	4.01
B	3.12	3.90

In order to evaluate the influence of a hydrogenated phase on the HPW adsorption, the hydrogen atoms were added to the face (001) of TT-Nb_2O_5, which presented the best result in our theoretical calculations. The results are described in Table 7.

Table 7. Relative adsorption energies (Er_{ads}), in kcal mol^{-1}, for the adsorbed HPW on phase TT (hydrogenated and dehydrogenated)

Phase TT	$Er_{ads}(pos1)$	$Er_{ads}(pos2)$
Hydrogenated	0	8.25
Dehydrogenated	9.93	25.83

Hydrogenated phases are characteristic of a treatment with a milder temperature, generating amorphous phases. According to the experimental values, mild treatments resulted in a better HPW adsorption, and this tendency is confirmed by means of our theoretical procedures. Once the HPW adsorption on the surface of hydrogenated TT-Nb_2O_5 phase happens, our findings point out lower energy values than those without the presence of hydroxyl groups.

Keeping in mind that the HPW adsorption on the catalyst surface is preferably in position 1, AIM calculations were performed in this system in order to assess the influence of the support on the acid character of the HPW hydrogens. The computed results by using the AIM methodology are described in Table 8. It is important to notice that for ionic character: DelSqRho > 0; –G/V > 1; G+V > 0 and for covalent character: DelSqRho < 0; –G/V < 1; G+V < 0. The more pronounced ionic character in the O-H bond of HPW is related to the higher acidity of this compound.

Table 8. Binding forces of acid protons on HPW in position 1 (G is the Kinetic Energy; V is the Potential Energy; DelSqRho is the Laplacian of Rho (electron density))

	DelSqRho	G+V	-G/V
HPW/H1	-1.5579	-0.4540	0.1245
HPW/H2	-1.5579	-0.4540	0.1245
HPW/H3	-1.5522	-0.4486	0.1189
Phase B/HPW/H1	-0.9588	-0.2861	0.1396
Phase B/HPW/H2	-1.0500	-0.3121	0.1372
Phase B/HPW/H3	-0.8880	-0.2560	0.1173
Phase T/HPW/H1	-1.5203	-0.4477	0.1312
Phase T/HPW/H2	-1.5622	-0.4600	0.1313
Phase T/HPW/H3	-1.7582	-0.5065	0.1167
Phase TT/HPW/H1	-1.7089	-0.5055	0.1341
Phase TT/HPW/H2	-1.8079	-0.5374	0.1372
Phase TT/HPW/H3	-2.6618	-0.7709	0.1203
Species**	DelSqRho	G+V	-G/V
Phase TT/HPW/H1	-1.5027	-0.4383	0.1250
Phase TT/HPW/H2	-1.4486	-0.4248	0.1285
Phase TT/HPW/H3	-1.4682	-0.4244	0.1191

*Dehydrogenated surfaces. **Hydrogenated surfaces.

AIM studies revealed that the O-H bond strength of the adsorbed acids decreases with increasing the crystallinity of the support. These results corroborate with the adsorption energy values, since the interaction between the oxygens on the surface and HPW is less intense in more crystalline phases, making the hydrogen more susceptible to react with isopropanol. Despite the higher acid character of the HPW hydrogens occurs under the influence of more crystalline supports, the low number of adsorbed molecules on their surfaces could, in principle, explain the lower performance of these catalysts experimentally.

According to the AIM calculations, the acidity of the HPW hydrogens increases with the crystallinity of the support. In phases of lower crystallinity, the hydrogens are more strongly bonded to the acid, but as the HPW adsorption is higher in these phases, there is a better catalytic performance. By analyzing the hydrogenated surfaces of phase TT, we also realized this tendency. As the adsorption was better on these surfaces, the covalent character increased according to the AIM calculations, in relation to the dehydrogenated phase TT.[62,63]

CONCLUSIONS

Our work corroborates the dropping method as efficient for the impregnation of HPW over niobia as shown by the analysis of the combination of the XRD, FT-IR, FT-Raman and ^{31}P NMR results obtained. The theoretical results point to the pseudo-hexagonal and

orthorhombic as the most likely crystalline forms for these catalysts calcinated at 600 °C in accordance with the XRD results and, also, suggest that the approach of HPW to the support positions the 3 acidic protons away from the OH groups of the niobia surface.

ACKNOWLEDGMENTS

The authors thank the Brazilian agencies CAPES (Science without Borders Program), CNPq (Grant Nº 308225/2018-0), FAPEMIG, FAPERJ (Grant Nº E-02/202.961/2017) for the financial support, the Brazilian Society of Mining and Metallurgy for the niobium oxide samples, and the Military Institute of Engineering and IRCELyon/CNRS for physical infrastructure. This work was also supported by Long-term development plan UHK.

REFERENCES

1. Keggin, J. F.; *Royal Soc.* **1934**, *144*, 75.
2. Kozhevnikov, V.; *Russ. Chem. Rev.* **1987**, *56*, 811.
3. Schwegler, M. A.; Vinke, P.; Van der Eijk, M.; Van Bekkum, H.; *Appl. Catal., A* **1992**, *80*, 41.
4. Okuhara, T.; Mizuno, N.; Misono, M.; *Adv. Catal*. **1996**, *41*, 113.
5. Yang, J.; Janik, M. J.; Ma, D.; Zheng, A.; Zhang, M.; Neurock, M.; Davis, R. J.; Ye, C.; Deng, F.; *J. Am. Chem. Soc.* **2005**, *127*, 18274.
6. Fernandes, S. A.; Cardoso, A. L.; Silva, M. J.; *Fuel Process. Technol.* **2012**, *96*, 98.
7. Mattos, F. C. G; Carvalho, E. N. C. B.; Freitas, E. F.; Paiva, M. F.; Ghesti, G. F.; Macedo, J. L.; Dias, S. C. L.; Dias, J. A.; *J. Braz. Chem. Soc.* **2017**, *28*, 336.
8. Freitas, E. F.; Araújo, A. A. L.; Paiva, M. F.; Dias, S. C. L.; Dias, J. A.; *Mol. Catal.* **2018**, *458*, 152.
9. Rafiee, E.; Eavani, S.; *RSC Adv.* **2016**, *6*, 46433.
10. Santos, F. M.; Nogueira, H. I. S.; Cavaleiro, A. M. V.; Gomes, E. M.; Belsley, M. S.; *Inorg. Chim. Acta* **2017**, *455*, 600.
11. Nico, C.; Monteiro, T.;Graça, M. P. F.; *Progr. Mat. Sci.* **2016**, *80*, 1.
12. Jacob, K. T.; Shekhar, C.; Vinay, M.; *J. Chem. Eng. Data* **2010**, *55*, 4854.
13. Bajuk-Bogdanovi, D., Popa, A.; Uskokovic-Markovic, S.; Holclajtner-Antunovic, I.; *Vibrat. Spectrosc.* **2017**, *92*, 151.
14. Wang, S. S.; Yang, G. Y.; *Chem. Rev.* **2015**, *115*, 4893.
15. Stawicka, K.; Sobczak, I.; Trejda, M. Sulikowski, B.; Ziolek, M.; *Microporous Mesoporous Mater.* **2012**, *155*, 143.
16. Mizuno, N.; Misono, M.; *Curr. Opin. Solid. Stat. Mat. Sci.* **1997**, *2*, 84.
17. Timofeeva, M. N.; *Appl. Catal., A* **2003**, *256*, 19.
18. Serwicka, E. M.; Grey, C. P.; *Colloid Surf.* **1990**, *45*, 69.
19. Jalil, P. A.; Faiz, M.; Tabet, N.; Hamdans, N. M.; Hussain, Z.; *J. Catal*. **2003**, *217*, 292.
20. Jalil, P. A.; Tabet, N.; Faiz, M.; Hamdan, N. M.; Hussain, Z.; *Appl. Catal., A* **2004**, *257*, 1.
21. Wu, Y.; Ye, X.; Yang, X.; Wang, X.; Chu, W.; Hu, Y.; *Ind. Eng. Chem. Res.* **1996**, *35*, 2546.
22. Vazquez, P. G.; Blanco, M. N.; Caceres, C. V.; *Catal. Lett.* **1999**, *60*, 205.
23. Pizzio, L. R.; Vazquez, P. G.; Caceres, C. V.; Blanco, M. N.; *Appl. Catal., A* **2003**, *256*, 125.
24. Pizzio, L. R.; Caceres, C. V.; Blanco, M. N.; *Appl. Catal., A* **1998**, *167*, 283.
25. Bielanski, A.; Lubanska, A.; Pozniczek, J.; Iiinicka, A. M.; *Appl. Catal., A* **2003**, *238*, 239.
26. Bielanski, A.; Lubanska, A.; Pozniczek, J.; Iiinicka, A. M.; *Appl. Catal. A* **2003**, *256*, 153.
27. Schwegler, M. A.; Vinke, P.; van der Eijk, M.; van Bekkum, H.; *Appl. Catal., A* **1992**, *80*, 41.
28. Dupont, P.; Vedrine, J. C.; Paumard, E.; Hecquet, G.; Lefebve, F.; *Appl. Catal., A* **1995**, *129*, 217.
29. Blasco, T.; Corma, A.; Martinez, A.; Martinez-Escolano, P.; *J. Catal*. **1998**, *177*, 306.
30. Nowinska, K.; Formaniak, R.; Kateta, W.; Waclaw, A.; *Appl. Catal., A* **2003**, *256*, 115.
31. Ivanov, A. V.; Zausa, E.; Taarit, Y. B.; Essayem, N.; *Appl. Catal., A* **2003**, *256*, 225.
32. Yadav, G. D.; Doshi, N. S.; *Catal. Today* **2000**, *60*, 263.
33. Yadav, G. D.; Doshi, N. S.; *Appl. Catal., A* **2002**, *236*, 129.
34. Yori, J. C.; Grau, J. M.; Benítez, V. M.; Sepúlveda, J.; *Appl. Catal., A* **2005**, *286*, 71.
35. Kozhevnikov, I. V.; Holmes, S.; Siddiqui, M. H.; *Appl. Catal., A* **2001**, *214*, 47.
36. Sharma, P.; Patel, A.; *Mater. Sci.* **2006**, *29*, 439.
37. Alsalme, A. M.; Wiper, P. V.; Khimyak, Y. Z.; Kozhevnikova, E. F.; Kozhevnikov, I. V.; *J. Catal.* **2010**, *276*, 181.
38. Balaraju, M.; Nikhitha, P.; Jagadeeswaraiah, K.; Srilatha, K.; Sai Prasad, P. S.; Lingaiah, N.; *Fuel Process Technol*. **2010**, *91*, 249.
39. Caliman, E.; Dias, J. A.; Dias, S. C. L.; Garcia, F. A. C.; Macedo, J. L.; Almeida, L. S.; *Microporous Mesoporous Mater.* **2010**, *132*, 103.
40. Kumar, R.; Gatla, S.; Mathon, O.; Pascarelli, S.; Lingaiah, N.; *Appl. Catal., A* **2015**, *502*, 297.
41. Bhattacharya, S.; Coasne, B.; Hung, F.R.; Gubbins, K. E.; *Stud. Surf. Sci. Catal.* **2007**, *160*, 527.
42. Tranca, D.C.; Wojtaszek-Gurdak, A.; Ziolek, M.; Tielens, F.; *Phys. Chem. Chem. Phys.* **2015**, *17*, 22401.
43. Weibin, Z.; Weidong, W.; Xueming, W.; Xinlu, C.; Dawei, Y.; Changle, S.; Liping, P.; Yuying, W.; Li, B.; *Surf. Interface Anal.* **2013**, *45*, 1206.
44. Derouane, E. G.; Védrine, J. C.; Pinto, R. R.; Borges, P. M.; Costa, L.; Lemos, M. A. N. D. A.; Lemos, F.; Ribeiro, F. R.; *Catal. Rev. Sci. Eng.* **2013**, *55*, 454.
45. Lacerda, C. V.; Barrios, A. C. M.; Sousa, R. R.; Franca, T. C. C.; Souza, R. O. L.; Gonzales, W. A.; Essayem, N.; Lachter, E. R.; *React. Kinet., Mech. Catal.* **2018**, *123*, 317.
46. te Velde, G.; Bickelhaupt, F. M.; Baerends, E. J.; Guerra, C. F.; van Gisbergen, S. J. A.; Snijders, J. G.; Ziegler, T.; *J. Comput. Chem.* **2001**, *22*, 931.
47. Srilatha, K.; Lingaiah, N.; Devi, B. L. A. P. R.; Prasad, B. N.; Venkateswar, S.; Prasad, P. S. S.; *Appl. Catal., A* **2009**, *365*, 28.
48. Albers, R. C.; Christensen, N. E.; Svane, A.; *J. Phys. Condens. Matter* **2009**, *21*, 343201.
49. Bader, R. F. W.; *Atoms in Molecules – A Quantum Theory*, Oxford University Press: Oxford, 1990, p. 458.
50. Matta, C. F.; *Struct. Chem.* **2017**, *28*, 1591.
51. Jehng, J.; Wachs, I. E.; *Chem. Mater*. **1991**, *3*, 100.
52. Kozhevnikov, I. V.; Kloetstra, K. R.; Sinnema, A.; Zandbergen, H. W.; Van Bekkum, H.; *J. Mol. Catal. A: Chem.* **1996**, *114*, 287.
53. Ushikubo, T.; Koike, Y.; Wada, K.; Xie, L.; Wang, D.; Guo, X.; *Catal. Today* **1996**, *28*, 59.
54. Khder, A. E. R. S.; Hassan, M. A. H.; El-Shall, M. S.; *Appl. Catal., A* **2014**, *487*, 110.
55. Maurer, S.; Ko, E. I.; *J. Catal.* **1992**, *135*, 125.
56. Paulis, M.; Martín, M.; Soria, D. B.; Díaz, A.; Odriozola, J. A.; Montes, M.; *Appl. Catal., A* **1999**, *180*, 411.
57. Janik, M. J.; Bardin, B. B.; Davis, R. J.; Neurock, M.; *J. Phys. Chem. B* **2006**, *110*, 4170.
58. Kozhevnikov, I. V.; Sinnema, A.; Jansen, R. J. J.; Van Bekkum, H.; *Catal. Lett.* **1994**, *27*, 187.
59. Essayem, N.; Tong, Y. Y.; Jobic, H.; Vedrine, J. C.; *Appl. Catal., A* **2000**, *194*, 109.
60. Uchida, S.; Inumaru, K.; Misono, M.; *J. Phys. Chem. B* **2000**, *104*, 8108.
61. Mastikhin, V. M.; Kulikov, S. M.; Nosov, A. V.; Kozhevnikov, I. V.; Mudrakovsky, I. L.; Timofeeva, M. N.; *J. Mol. Catal*. **1990**, *60,* 65.
62. Mesquita, A. M.; Guimaraes, I. R.; de Castro, G. M. M.; Goncalves, M. A.; Ramalho, T. C.; Guerreiro, M. C.; *Appl. Catal., B* **2016**, *192*, 286.
63. Ramalho, T. C.; Buhl, M.; *Mag. Res. Chem.* **2005**, *43*, 139.